

Decay dynamics of the positively charged exciton in a single charge tunable self-assembled quantum dot

P. A. Dalgarno,^{a)} J. McFarlane, B. D. Gerardot, and R. J. Warburton
*School of Engineering and Physical Sciences, Heriot-Watt University, Edinburgh EH14 4AS,
 United Kingdom*

K. Karrai
Center for NanoScience, LMU, Geschwister-Schooll-Platz 1, 80539 Munich, Germany

A. Badolato and P. M. Petroff
Materials Department, University of California, Santa Barbara, California 93106

(Received 17 April 2006; accepted 3 June 2006; published online 24 July 2006)

We report on the decay dynamics of positively charged excitons confined to single InAs quantum dots embedded in an *n*-type field-effect structure. The positively charged exciton's dynamics are found to be strongly dependent on device dimensions. With a large (small) dot capping layer the decay is dominated by hole tunneling (radiative recombination). The hole tunneling is successfully modeled with a WKB-like zero-dimensional to three-dimensional tunneling approximation. Hole tunneling is not observed in the dynamics of the neutral exciton negatively charged exciton, or biexciton, an effect we attribute to an increase in barrier height through the interdot Coulomb interactions. © 2006 American Institute of Physics. [DOI: 10.1063/1.2234745]

Self-assembled quantum dots are potential candidates for many novel optoelectronic and photonic applications due to their zero-dimensional density of states and the ease with which the dots can be incorporated into semiconductor heterostructures. Positioning dots within the active region of an *n*-Schottky or *p*-Schottky photodiode allows for the manipulation of dot charge,¹ a technique used to realize quantum dot spin memory,² electrically driven single photon emission,³ and an optically triggered single electron turnstile.⁴ Carrier tunneling plays a key role in the operation of such Schottky devices. For example, in an *n*-type device electron tunneling can be used to control exciton charge,⁵ whereas in a *p*-type device hole tunneling can potentially be used to probe the spin of the electron in the dot.

In this letter we show that the recombination dynamics of excitons confined to dots in an *n*-type device are strongly influenced by hole tunneling. We establish control of hole tunneling through the applied field, dot charge, and device dimensions.

The dots studied are annealed InAs/GaAs self-assembled dots grown embedded in a metal-insulator-semiconductor field-effect device (Fig. 1). An *n*-type ($\sim 10^{18} \text{ cm}^{-3}$) GaAs back contact is separated from the dots by a 25 nm GaAs tunneling barrier. A GaAs capping layer of 30 nm (sample A) or 10 nm (sample B) then separates the dots from an AlAs/GaAs blocking barrier. The blocking barrier prevents carrier leakage to a NiCr Schottky gate evaporated onto the sample surface. A bias applied between the Schottky gate and the back contact moves the dot level with respect to the Fermi level in the back contact. Electrons tunnel from the back contact in and out of the dot when the dot levels are resonant with the Fermi level. The pronounced Coulomb blockade of the dots gives rise to single electron control over the charging. Nonresonant optical excitation is used to form excitons with either a single hole or two holes.

The photoluminescence (PL) from a single dot is probed by using a diffraction-limited confocal microscope and a sample with a dot density of less than 1 dot/ μm^2 . A glass, $n=2.0$, half-spherical solid immersion lens is used to reduce the collection spot size to $\sim 380 \text{ nm}$ at the dot emission wavelength ($\sim 950 \text{ nm}$), which in turn increases collection efficiency by a factor of ~ 5 .

Decay dynamics are studied using time resolved PL (TRPL). Carriers are excited in the wetting layer of the dots using an 826 nm, 100 ps pulsed laser diode, and time correlated single photon counting (TCSPC) is performed using a silicon single photon avalanche photodiode. The system's temporal resolution is 400 ps, but iterative convolution is used to extract lifetimes with an accuracy of 100 ps. The avalanche diode, collects photoluminescence from a spectral window of 0.5 meV, smaller than the energy differences between the PL from different excitons in the same dot, which are typically greater than 1 meV. The spectral resolution of the TRPL system therefore allows for the collection of PL from a chosen single exciton line from a single dot.

Figure 2(a) shows the photoluminescence as a function of applied bias from a single dot from sample A. Clear jumps are seen in the PL corresponding to the loading of single electrons from the back contact into the dots. The neutral exciton X^0 , singly negatively charged exciton X^{1-} , singly positively charged exciton X^{1+} , and biexciton $2X^0$ are

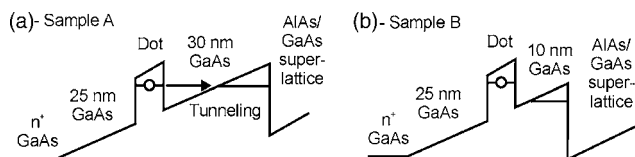


FIG. 1. (a) Schematic of the valence band potential profile of sample A. The interface between the GaAs capping layer and the superlattice forms a triangular well. Holes can tunnel from the dots to this well. (b) Schematic of sample B. Reducing the dot capping layer to 10 nm raises the triangular well states to a higher energy than the hole states in the dot, preventing hole tunneling.

^{a)}Electronic mail: p.a.dalgarno@hw.ac.uk

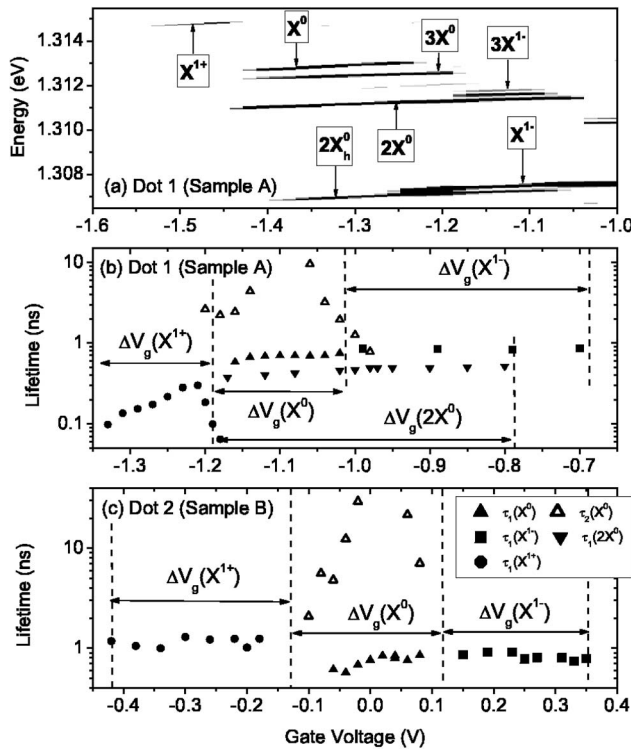


FIG. 2. (a) Gray scale plot of the time-integrated PL from a single dot from sample A at 5 K. White (black) corresponds to 80 (2000) counts. (b) The measured lifetime over the gate voltage plateau of X^{1+} , X^0 , $2X^0$, and X^{1-} for the dot shown in (a). ΔV_g shows the gate voltage extent of each exciton plateau. X^{1+} is the only exciton for which the lifetime shows an asymmetric gate voltage dependence with respect to the center of the gate voltage plateau. (c) The measured lifetime of X^{1+} , X^0 , and X^{1-} for a single dot from sample B. Note that there is no longer a voltage dependence for the X^{1+} lifetime.

labeled.^{5,6} The remaining lines arise from exciton complexes containing more than two holes and hot hole excitons. Figure 2(b) shows the radiative lifetime of X^0 , $2X^0$, X^{1-} , and X^{1+} for the dot shown in Fig. 2(a). Example decay curves from each exciton are shown in Fig. 3. There is a shift in the gate voltages at which charging events occur in Fig. 2(a) and 2(b) due to a power dependent formation of a positive space charge region in the device.⁷

The TRPL from X^{1-} and $2X^0$ show single, bias independent lifetimes of 0.86 and 0.46 ns, respectively. The bias independence of these lifetime implies that the lifetimes correspond directly to the radiative lifetime. Nonradiative decay, in the form of carrier tunneling, would be expected to show a field dependence as the tunneling barriers surrounding the dot alter with field. Similar lifetime results have been reported for InAs self-assembled dots without a charge tunable structure⁸ and agree with the known dot oscillator strength.⁹ The TRPL from X^0 shows two lifetime components, a bias

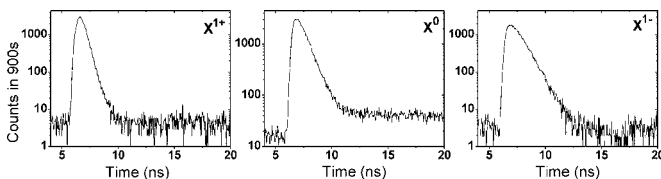


FIG. 3. PL decay curves data for X^{1+} , X^0 , and X^{1-} for the dot shown in Fig. 2(a). The data are taken from the center of each exciton's voltage plateau. The slow X^0 decay corresponds to a tertiary decay component, not shown in Fig. 2(b), whose origin is presently unknown.

independent lifetime of 0.7 ns and a highly bias dependent lifetime, symmetric around the center of the X^0 voltage plateau, ranging from 0.7 to 9 ns. The bias independent lifetime is the radiative lifetime, with similar magnitude to X^{1-} . The bias dependent lifetime arises due to the fine structure of X^0 . Nonresonant excitation leads to the formation of either radiative or nonradiative neutral excitons. The electron in the nonradiative exciton undergoes a spin flip, turning the exciton radiative, through a Kondo-like spin-swap interaction with an electron in the back contact.¹⁰

The decay dynamics of X^{1+} are considerably different from all other excitons from dots in sample A. There is a single decay component with a strong bias dependence. At gate voltages greater than -1.22 V, the lifetime decreases rapidly from 0.6 to 0.31 ns over a voltage range of 20 mV. At these voltages X^{1+} charges to $2X^0$ and the rapid decrease in the X^{1+} lifetime corresponds to the rapid electron tunneling from the back contact into the dot. At gate voltages below -1.22 V the lifetime decreases with decreasing voltage, from 0.3 to 0.1 ns over a range of 130 mV. The integrated intensity of X^{1+} (not shown) shows a similar gate voltage behavior. This voltage dependence of both the lifetime and intensity is unique to X^{1+} and is absent in the decay dynamics measured from all other excitons in sample A, a result we have verified by studying over ten dots from the same sample.

In understanding the decay dynamics of X^{1+} the field dependence is the key. As previously discussed radiative recombination should show no field dependence implying that the dynamics of X^{1+} are dominated by carrier tunneling. At gate voltages a few millivolts away from the charging events between excitons the energy difference between the exciton in the dot and any other charged exciton is far greater than $k_B T$ at 5 K. This prohibits the tunneling of electrons from the back contact into the dots and implies that the lifetime behavior is therefore due to hole tunneling. This necessitates the existence of a nearby hole continuum. Such a continuum is available in the form of a two-dimensional (2D) triangular well formed where the capping layer of the dots meets the blocking barrier of the device [Fig. 1(a)].^{7,11}

Tunneling from the dots to this continuum occurs through a triangular barrier and is modeled using a zero-dimensional (0D) to three-dimensional (3D) WKB-like approximation.¹² This model approximated the dot confinement in the growth direction with a one-dimensional (1D) square well of width L , corresponding to the dot effective height, and depth V_w . The tunneling time τ_{tun} is given by

$$\frac{1}{\tau_{\text{tun}}} = \left(\frac{4V_w}{\pi\hbar} \right)^2 \sqrt{\frac{L^2 m_h^*}{2E_v}} \exp \left[\frac{-4}{3\hbar e F} \sqrt{2m_h^* E_v^3} \right]. \quad (1)$$

L is known to be approximately 3 nm from atomic force microscopy (AFM)¹³ and cross-sectional scanning tunneling microscopy (X-STM) work on similar dots. m_h^* is taken to be $0.25m_0$.¹⁵ E_v is the ionization energy of a single hole in the dot. E_v and L can be used to determine the well depth V_w using a simple 1D finite square well model. F is the applied field, calculated using the device dimensions and the applied bias through the so-called lever arm relationship, taking into account the Schottky barrier height, 0.6 eV,¹⁵ and compensating for power dependent hole accumulation in the device.⁷ F is therefore bias dependent, decreasing the lifetime with increasing reverse bias, as seen in the experimental data.

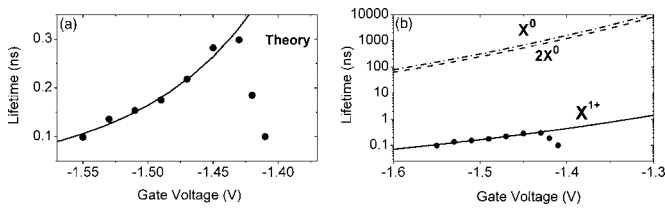


FIG. 4. (a) X^{1+} lifetime data and WKB-like calculation of the hole tunneling for X^{1+} for dot 1 from sample A. (b) shows the same result as (a) with the added WKB-like calculation for the calculated hole tunneling for X^0 and $2X^0$. The ionization energies used in the calculations are shown in Table I.

The uniqueness of the X^{1+} decay dynamics is found to be due to the dependence of E_v on dot charge. This dependence is due to the pronounced Coulomb interactions between carriers in the dots.¹⁵ With only a single hole in the dot, E_v is defined by the confinement potential of the dot and labeled E_v^0 . For X^{1+} E_v is increased by the electron-hole Coulomb energy E_{ch} and decreased by the hole-hole Coulomb energy E_{hh} . For all cases E_{hh} is greater than E_{ch} , leading to a net decrease of E_v compared to E_v^0 . The gate voltage extents of each exciton plateau and the energy shifts upon charging are used to determine the Coulomb energies and the single hole ionization energies.^{6,11} For the dot shown in Figs. 2(a) and 2(b) the calculated energies are shown in Table I.

Figure 4(a) shows the result from applying Eq. (1) to the X^{1+} data presented in Fig. 2(b). There are no fitting parameters: all terms are known either from the sample dimensions or through the Coulomb model. The theory shows excellent agreement with the data, despite the sensitivity of the tunneling time to the parameters, verifying that the decay dynamics of X^{1+} is dominated by hole tunneling. We note that a simple 1D WKB approximation¹⁶ produces an equally high quality fit using $E_v^0=75$ meV, which is within the estimated error of the ionization energy from the Coulomb model. Strictly, we have a 2D continuum, and it has been previously shown that hole tunneling can be suppressed away from resonances between the dot level and the hole level in the 2D well.¹¹ However, the strong agreement between experiment and theory implies that we are close to a tunneling resonance in this experiment.

The data presented in Fig. 2(b) show that the decay dynamics of X^0 , X^{1-} , and $2X^0$ are not influenced at all by tunneling. E_v for X^0 , X^{1-} , and $2X^0$ are all increased by the Coulomb interactions, as shown in Table I. Figure 4(b) shows the calculated hole tunneling time for X^0 and $2X^0$. The WKB-like approximation predicts hole tunneling times far greater than the radiative lifetime of each exciton. This shows that

TABLE I. The hole ionization energies E_v for X^{1+} , $2X^0$, X^0 , and X^{1-} in terms of the Coulomb energies and the single particle ionization energy E_v^0 . The Coulomb energies and E_v^0 are calculated for the dot shown in Fig. 1(a) from the Coulomb blockade model (Ref. 5). For $E_v=85$ meV and $L=3$ nm, V_w is determined to be 140 meV.

| Exciton | X^{1+} | X^0 | $2X^0$ | X^{1-} |
|--------------|---------------------------|------------------|----------------------------|-------------------|
| E_v (meV) | $E_v^0 + E_{ch} - E_{hh}$ | $E_v^0 + E_{ch}$ | $E_v^0 + 2E_{ch} - E_{hh}$ | $E_v^0 + 2E_{ch}$ |
| Term | E_v^0 | E_{ec} | E_{ch} | E_{hh} |
| Energy (meV) | 85 | 26.6 | 32 | 33 |

hole tunneling can be successfully switched off through charging the device.

We are able to provide strong verification of our interpretation through measurements on sample B. Altering the capping layer thickness has a profound effect on the tunneling dynamics of X^{1+} . Figure 2(c) shows lifetime data for X^0 , X^{1-} , and X^{1+} from a single dot from sample B. The decay dynamics from X^0 and X^{1-} are similar to sample A. The decay dynamics of X^{1+} show a constant lifetime of ~ 1 ns and no bias dependence. The reduced capping layer increases the energy level of the well states at the interface relative to the hole states in the dot [Fig. 1(b)]. By approximating the energy levels in the triangular interface with a simple 2D triangular well model¹¹ we determine that the hole level in the dot is 30 meV lower in energy than the lowest available level in the 2D well. Tunneling is therefore no longer a possible decay path for the holes in the dot and has consequently been turned off through the reduction of the capping layer.

In conclusion we have shown that the decay dynamics of the positively charged exciton in a single n -type charge tunable dot show pronounced effects due to hole tunneling. The nature of this tunneling can be accurately predicted by applying a 0D–3D WKB-like tunneling approximation. The hole tunneling can be turned off through charging the dot due to the change in Coulomb interactions within the dot. The hole tunneling can also be turned off by reducing the capping layer of the dots.

¹R. J. Warburton, C. S. Dürr, K. Karrai, J. P. Kotthaus, G. Medeiros-Ribeiro, and P. M. Petroff, Phys. Rev. Lett. **79**, 5282 (1997).

²M. Kroutvar, Y. Ducommun, D. Heiss, M. Bichler, D. Schuh, G. Abstreiter, and J. J. Finley, Nature (London) **432**, 81 (2004).

³Z. L. Yuan, B. E. Kardynal, R. M. Stevenson, A. J. Shields, C. J. Lobo, K. Cooper, N. S. Beattie, D. A. Ritchie, and M. Pepper, Science **295**, 102 (2002).

⁴A. Zrenner, E. Beham, S. Stuffer, F. Findeis, M. Bichler, and G. Abstreiter, Nature (London) **418**, 612 (2002).

⁵R. J. Warburton, C. Schafflein, D. Haft, F. Bickel, A. Lorke, K. Karrai, J. M. Garcia, W. Schoenfeld, and P. M. Petroff, Nature (London) **405**, 926 (2000).

⁶M. Ediger, P. A. Dalgarno, J. M. Smith, B. D. Gerardot, R. J. Warburton, K. Karrai, and P. M. Petroff, Appl. Phys. Lett. **86**, 211909 (2005).

⁷J. M. Smith, P. A. Dalgarno, B. Urbaszek, E. J. McGhee, G. S. Buller, G. J. Nott, and R. J. Warburton, Appl. Phys. Lett. **82**, 3761 (2003).

⁸C. Santori, G. S. Solomon, M. Pelton, and Y. Yamamoto, Phys. Rev. B **65**, 073310 (2002).

⁹A. Högele, S. Seidl, M. Kroner, K. Karrai, R. J. Warburton, B. D. Gerardot, and P. M. Petroff, Phys. Rev. Lett. **93**, 217401 (2004).

¹⁰J. M. Smith, P. A. Dalgarno, R. J. Warburton, A. O. Govorov, K. Karrai, B. D. Gerardot, and P. M. Petroff, Phys. Rev. Lett. **94**, 197402 (2005).

¹¹S. Seidl, P. A. Dalgarno, M. Kroner, J. M. Smith, A. Högele, M. Ediger, B. D. Gerardot, J. M. Garcia, P. M. Petroff, K. Karrai, and R. J. Warburton, Phys. Rev. B **72**, 195339 (2005).

¹²J. M. Villas-Boas, S. E. Ulloa, and A. O. Govorov, Phys. Rev. Lett. **94**, 057404 (2005).

¹³D. Granados and J. M. Garcia, Appl. Phys. Lett. **82**, 2401 (2003).

¹⁴Q. Gong, P. Offermans, R. Notzel, P. M. Koenraad, and J. H. Wolter, Appl. Phys. Lett. **85**, 5697 (2004).

¹⁵R. J. Warburton, B. T. Miller, C. S. Dürr, C. Bodefeld, K. Karrai, J. P. Kotthaus, G. Medeiros-Ribeiro, P. M. Petroff, and S. Huant, Phys. Rev. B **58**, 16221 (1998).

¹⁶P. W. Fry, J. J. Finley, L. R. Wilson, A. Lemaitre, D. J. Mowbray, M. S. Skolnick, M. Hopkinson, G. Hill, and J. C. Clark, Appl. Phys. Lett. **77**, 4344 (2000).